TUM-HEP 695/08

A note on the primordial abundance of stau NLSPs

Michael Ratz[1], **Kai Schmidt-Hoberg**[2] **and Martin Wolfgang Winkler**[3]

Physik-Department T30, Technische Universität München,
James-Franck-Straße, 85748 Garching, Germany

Abstract

In scenarios with a gravitino LSP, there exist strong BBN constraints on the abundance of a possible stau NLSP. We find that in settings with substantial left-right mixing of the stau mass eigenstates these constraints can be evaded even for very long-lived staus.

[1]Email: mratz@ph.tum.de
[2]Email: kschmidt@ph.tum.de
[3]Email: mwinkler@ph.tum.de

1 Introduction

Arguably, supersymmetry (SUSY) is one of the most plausible extensions of the standard model (SM). Apart from its theoretical appeal, SUSY has the virtue of providing a compelling dark matter candidate, the lightest supersymmetric particle (LSP), which is stable if R parity is conserved. A particular interesting dark matter candidate is the gravitino, which evades direct detection because all its interactions are suppressed by the Planck scale. The hypothesis of a gravitino LSP may nevertheless be tested at the LHC if certain conditions are met. First, the next-to-lightest supersymmetric particle (NLSP) has to be charged, and second the gravitino mass may not be too small. In this case, one could observe long-lived charged particles in whose decays one could probe the properties of the LSP [1–4]. The collider phenomenology of such scenarios has been explored in various studies [1–9].

There are several theoretical reasons which make it appear desirable to have gravitino masses $m_{3/2}$ not much smaller than the masses of the SM superpartners. For instance, simple explanations of the μ and $B\,\mu$ terms seem to require not too small $m_{3/2}$ [10, 11]. Further, many simple mechanisms of baryogenesis, in particular leptogenesis [12], need rather high reheating temperatures T_R [13] which can be achieved for gravitino masses of about $10 \ldots 100\,\mathrm{GeV}$ [14, 15] (i.e. at least the constraints from gravitino overproduction can be satisfied).

However, there are severe constraints on such scenarios coming from cosmology. The observed primordial abundances of light elements produced in big bang nucleosynthesis (BBN) allow to place stringent constraints on the number density of long-lived particles whose decays happen during or after BBN and induce nuclear reactions that change the element abundances [16–18]. While a neutralino NLSP is strongly disfavored for gravitino masses in the GeV range [3,19], scenarios with a sneutrino NLSP are essentially unconstrained but very hard to test experimentally [20, 21]. This makes a charged slepton, specifically a stau, particularly appealing as an NLSP candidate. The stau NLSP abundance and lifetime can satisfy the limits obtained from BBN by considering NLSP decays alone [22,3, 15, 19, 23–28]. However, as pointed out in [29], charged NLSPs form bound states with light nuclei, which leads to a drastic overproduction of ^{6}Li. This process, known as Catalyzed BBN (CBBN), leads to strong constraints on the stau relic abundance, unless the NLSP lifetime is shorter than a few thousand seconds.

Several ways to circumvent BBN constraints have been discussed in the literature. For instance, entropy production between NLSP freeze-out and the start of BBN can dilute the NLSP abundance sufficiently to satisfy all constraints even for long lifetimes [15,30,31]. However, in order to arrive at such scenarios one usually relies on new sectors which are typically very hard to access experimentally. Alternatively, the NLSP can be sufficiently short lived if the gravitino is very light, R parity is slightly broken [32, 33] or the superpartner mass spectrum is sufficiently heavy [34]. However in these cases it is practically impossible to test the nature of the LSP.

The purpose of this study is to point out that there are regions within the parameter space of the minimal supersymmetric extension of the standard model (MSSM) where the relic stau abundance is strongly suppressed such that the bounds from CBBN can

be evaded even for long stau lifetimes. As we shall see, small thermal relic abundances of staus occur in parameter regions with a substantial left-right mixing of the stau mass eigenstates, where the annihilation into Higgs bosons is greatly enhanced.

The paper is organized as follows. In the next section we will introduce the stau-Higgs coupling and calculate the Higgs channel cross section. Section 3 is devoted to a discussion of theoretical constraints on trilinear couplings between Higgs and $\widetilde{\tau}$ fields. In Section 4 we review the relevant BBN constraints and discuss the stau relic abundance. Continuing with Section 5 we introduce three scenarios within the MSSM in which a strong suppression of the stau relic abundance can be achieved such that all cosmological constraints can be evaded. Finally in Section 6 we briefly discuss the implications of our scenario for the LHC.

2 Annihilation into Higgs bosons

In the early universe, superpartners are copiously produced; usually they are assumed to be in thermal equilibrium. As the universe cools down, they will cascade into staus, which we assume to be the NLSPs. Since staus are metastable, until the BBN era their abundance will only decrease due to annihilation. In most analyses performed so far, the lightest stau is assumed to be purely right-handed. Then, for its freeze-out, only electroweak annihilation processes have to be considered. The couplings governing the relevant reactions are either the electric charge e or the $\mathrm{U}(1)_Y$-coupling $g_Y = e/\cos\theta_\mathrm{W}$, where θ_W denotes the Weinberg angle. These couplings are rather small, leading to a relatively large stau abundance after freeze-out [22],

$$Y_{\widetilde{\tau}_\mathrm{R}} \gtrsim 10^{-13} \quad \text{for} \quad m_{\widetilde{\tau}_1} \gtrsim 100\,\mathrm{GeV}\,, \tag{1}$$

where the abundance $Y \equiv n/s$ is defined as the ratio of number and entropy densities. Such a large relic stau abundance is allowed by CBBN only if the gravitino is very light and the stau lifetime accordingly short. If the lighter stau has a left-handed component, the electroweak annihilation cross section gets enhanced due to its $\mathrm{SU}(2)_\mathrm{L}$ couplings, but as CBBN bounds are very tight, the inclusion of further gauge interactions changes the situation only marginally. On the other hand, we shall see that in the case of substantial left-right mixing in the stau sector, the couplings between staus and Higgs bosons can get significantly enhanced, thus greatly suppressing the stau relic abundance.

2.1 Coupling of staus to Higgs bosons

To find the regions of parameter space where this annihilation reaction is important, we now turn to the Lagrangean term which describes the couplings between the light stau and the light Higgs. In our analytic discussion, we make a couple of simplifying assumptions; later, in Section 5, we will take into account all interactions and states.

We shall assume that there is no generation mixing in the slepton sector which is suggested by flavor constraints. Furthermore we take μ and A^τ to be real parameters.

Then the relevant terms read[1]

$$\begin{aligned}\mathscr{L}_{\widetilde{\tau}_1\widetilde{\tau}_1 h} &= \frac{g_2}{2M_W}\Big\{M_W^2\,\sin(\alpha+\beta)\,\left[\left(\tan^2\theta_{\rm W}-1\right)\,\cos^2\theta_{\widetilde{\tau}}-2\tan^2\theta_{\rm W}\,\sin^2\theta_{\widetilde{\tau}}\right] \\ &\quad + m_\tau\,\frac{\mu\,\cos\alpha - A^\tau\,\sin\alpha}{\cos\beta}\sin 2\theta_{\widetilde{\tau}} + 2m_\tau^2\,\frac{\sin\alpha}{\cos\beta}\Big\}\;h\,\widetilde{\tau}_1^+\widetilde{\tau}_1^- \;. \qquad (2)\end{aligned}$$

For simplicity we assume that the Higgs bosons except h be relatively heavy ($\gtrsim 300$GeV), which is the case for all models we are considering later. This allows us to work in the 'decoupling limit' where the mixing parameter α can be written as $\alpha \simeq \beta - \pi/2$ and therefore $\cos\alpha \simeq \sin\beta$ and $\sin\alpha \simeq -\cos\beta$. The leading term of the Lagrangean which couples the lightest stau to the Higgs is then given by

$$\begin{aligned}\mathscr{L}_{\widetilde{\tau}_1\widetilde{\tau}_1 h} &= \frac{g_2}{2M_W}\,\sin 2\theta_{\widetilde{\tau}}\,m_\tau\,\left\{\mu\,\tan\beta + A^\tau\right\}\,h\,\widetilde{\tau}_1^+\widetilde{\tau}_1^- \\ &= -\frac{g_2}{2M_W}\,\sin 2\theta_{\widetilde{\tau}}\,m^2_{\widetilde{\tau}_{\rm LR}}\,h\,\widetilde{\tau}_1^+\widetilde{\tau}_1^- \;. \qquad (3)\end{aligned}$$

Here $m^2_{\widetilde{\tau}_{\rm LR}}$ denotes the off-diagonal element of the 2×2 stau mass matrix (cf. Appendix A).

2.2 Higgs channel cross section

With the stau-Higgs coupling (3), we can now calculate the cross section for the annihilation of the light staus into light Higgs bosons,

$$\widetilde{\tau}_1^+ + \widetilde{\tau}_1^- \;\to\; h + h \;. \qquad (4)$$

The contributing Feynman diagrams are shown in Figure 1. In our approximation, we

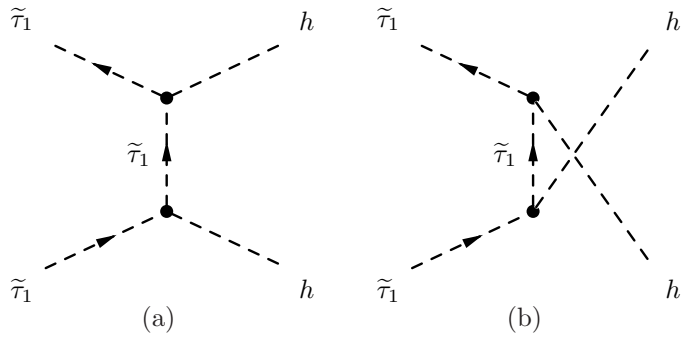

Figure 1: Stau annihilation into Higgs bosons.

consider only the exchange of $\widetilde{\tau}_1$, neglecting the exchange of $\widetilde{\tau}_2$. In zeroth order of a

[1]There exist different sign conventions for the A-parameter. Here we follow [35].

velocity expansion, the thermally averaged annihilation cross section $\langle \sigma_{\rm ann}\, v\rangle$ is equal to the cross section $\sigma_{\rm ann}$ times the relative velocity $v_{\rm rel}$ of the incoming staus. We obtain

$$\langle \sigma_{\rm ann}\, v\rangle \;\simeq\; \sigma_{\rm ann}\, v_{\rm rel} \;=\; \frac{1}{16\pi}\left(\frac{g_2}{2M_W}\,\sin 2\theta_{\widetilde\tau}\, m^2_{\widetilde\tau_{\rm LR}}\right)^4 \frac{\sqrt{m^2_{\widetilde\tau_1}-m_h^2}}{m^3_{\widetilde\tau_1}(2m^2_{\widetilde\tau_1}-m_h^2)^2}\,. \tag{5}$$

Clearly, this annihilation cross section becomes important for sizable left-right mixing and relatively small stau masses.

2.3 Comparison with electromagnetic cross section

It is instructive to compare the cross section (5) with a typical electroweak cross section. For example the annihilation cross section of staus into photons is given by [22] $\langle \sigma_{{\rm ann}\,\widetilde\tau^+\widetilde\tau^-\to\gamma\,\gamma}\, v\rangle \simeq 4\pi\alpha^2/m^2_{\widetilde\tau_1}$. If $m_{\widetilde\tau_1}$ and m_h are not too close, one has

$$\frac{\langle \sigma_{{\rm ann}\,\widetilde\tau^+\widetilde\tau^-\to h\,h}\, v\rangle}{\langle \sigma_{{\rm ann}\,\widetilde\tau^+\widetilde\tau^-\to\gamma\,\gamma}\, v\rangle} \;\sim\; \left(\frac{\tan\beta}{50}\right)^4 \left(\frac{\mu_{\rm eff}}{2m_{\widetilde\tau_1}}\right)^4\,, \tag{6}$$

where $\mu_{\rm eff}=\mu\,\sin 2\theta_{\widetilde\tau}$. Hence, for $\mu_{\rm eff} > 2m_{\widetilde\tau_1}$ the annihilation cross section is dominated by the Higgs channel. Even for an order one ratio $\mu_{\rm eff}/2m_{\widetilde\tau_1}$ one obtains a dramatic reduction of the primordial stau abundance. However, as we shall discuss next, there are constraints on the ratio $\mu_{\rm eff}/2m_{\widetilde\tau_1}$, implying that the reduction cannot be arbitrarily strong.

3 Theoretical constraints on μ

The enhancement of the stau annihilation cross section relies on a large trilinear Higgs-stau coupling, which might lead to an unwanted (color and) charge breaking (CCB) minimum of the potential. Such minima might be acceptable if the 'physical' vacuum is sufficiently long-lived. In what follows, we will first analyze the tree-level potential and see that in the interesting regions of parameter space there is indeed an unphysical minimum. We will discuss tunneling to this vacuum. Then we will discuss quantum corrections to the potential and see that they lift the unwanted minimum and possibly even make it disappear. Finally, we will comment on constraints on μ arising from unitarity.

3.1 CCB constraints at tree level

The relevant field space is given by two real fields, $\widetilde\tau = \frac{1}{\sqrt{2}}{\rm Re}(\widetilde\tau_1)$ and h. The corresponding scalar potential around the electroweak vacuum can be written as

$$V \;=\; \frac{1}{2}m^2_{\widetilde\tau_1}\,\widetilde\tau^2 + \frac{1}{2}m_h^2\,h^2 + b_h\,h^3 + b_{\widetilde\tau\widetilde\tau h}\,h\,\widetilde\tau^2 + \lambda_h\,h^4 + \lambda_{\widetilde\tau}\,\widetilde\tau^4 + \lambda_{\widetilde\tau h}\,\widetilde\tau^2\,h^2\,, \tag{7}$$

where at tree level $m_h \simeq 90\,\text{GeV}$, $b_h \simeq 17\,\text{GeV}$, $\lambda_h \simeq \lambda_{\widetilde{\tau}h} \simeq 0.018$, $\lambda_{\widetilde{\tau}} \simeq 0.028$ and the trilinear coupling $b_{h\widetilde{\tau}\widetilde{\tau}} = -\frac{y_\tau}{\sqrt{8}}\mu_{\text{eff}}$. For very negative $b_{h\widetilde{\tau}\widetilde{\tau}}$ values there is a second minimum of the tree-level potential. We have searched for minimal paths connecting the electroweak vacuum with the second, deeper minimum. It turns out that the relevant field direction is always very close to $x = \frac{1}{\sqrt{2}}(\widetilde{\tau} + h)$. The corresponding potential along that direction can be written as

$$V \;=\; \frac{1}{4}(m^2_{\widetilde{\tau}_1} + m^2_h)\, x^2 + \left(\frac{b_h}{\sqrt{8}} - y_\tau \frac{\mu_{\text{eff}}}{8}\right) x^3 + \frac{1}{4}(\lambda_h + \lambda_{\widetilde{\tau}} + \lambda_{h\widetilde{\tau}})\, x^4 \,. \tag{8}$$

In order to check whether the lifetime of the local minimum at $x = 0$ exceeds the age of the universe we have to calculate the so called bounce action S_{B} along the lines of [36], which should satisfy $S_{\text{B}} \geq 400$ [37]. Using the potential (8) with the coefficients given by their tree-level values we find an upper bound on the coefficient of the trilinear term $|\frac{b_h}{\sqrt{8}} - \frac{\mu_{\text{eff}}}{16}| \lesssim 33.5\,\text{GeV}$, which translates into

$$\mu_{\text{eff}} \;\lesssim\; 630\,\text{GeV} \quad (\text{for } \tan\beta = 50 \text{ and } m_{\widetilde{\tau}_1} = 120\,\text{GeV}) \,. \tag{9}$$

Note that for $\mu_{\text{eff}} \lesssim 430\,\text{GeV}$ the tree-level potential does not exhibit a second, deeper minimum at all.

3.2 Quantum corrections to CCB constraints

It is well known that quantum corrections can change the tree-level picture drastically. In order to analyze the situation properly, one has to take into account radiative corrections to the potential. This is a very complicated issue, and we refrain from performing a complete analysis here. In order to get a feeling for the impact of radiative corrections we include the standard stop loop correction (cf. e.g. [35, p. 245 f.]). The resulting effective potential is significantly steeper in the Higgs direction, such that the physical Higgs mass can violate the tree-level bound $m_h \leq m_Z$. It also turns out that the cubic and quartic coefficients in the Higgs potential get enhanced by $\sim 70\,\%$ and $\sim 40\,\%$, respectively. This has important implications for the bounce action: plugging the loop corrected values for these parameters into (8) we find that the metastable minimum has a sufficiently large lifetime for

$$\mu_{\text{eff}} \;\lesssim\; 780\,\text{GeV} \quad (\text{for } \tan\beta = 50 \text{ and } m_{\widetilde{\tau}_1} = 120\,\text{GeV}) \,. \tag{10}$$

The second, deeper minimum exists only if $\mu_{\text{eff}} \gtrsim 500\,\text{GeV}$.

There are similar effects, in particular for the potential in $\widetilde{\tau}$ direction. This issue has been studied in [38], where it was found that there are no charge breaking minima at all after quantum corrections are taken into account. Whether or not these statements also apply to parameter regions with large $\tan\beta$ and μ_{eff} will be studied elsewhere.

3.3 Unitarity bound

Further constraints on μ_{eff} come from unitarity. The unitary cross section for scalar particles can be calculated using partial wave expansion. In the case of a non-elastic

process it takes the form [39]

$$\sigma_{\text{unit}} \;=\; \frac{4\pi(2J+1)}{|\vec{p}_{\text{in}}|^2}\,, \tag{11}$$

where J is the angular momentum of the partial wave and $\vec{p}_{\text{in}}$ is the three-momentum of one incoming particle. The dominant contribution to the stau annihilation into Higgs bosons comes from s-wave scattering. Therefore the perturbative unitarity constraint relevant to our discussion is

$$\sigma_{\text{ann}\,\tilde{\tau}^+\tilde{\tau}^-\to h\,h} \;\leq\; \sigma_{\text{unit},s} \;=\; \frac{4\pi}{|\vec{p}_{\text{in}}|^2}\,. \tag{12}$$

If the bound is not respected, this signals that the perturbative calculation of the cross section is no longer valid. In our case, the unitarity bound translates into a constraint on the μ parameter. The bound is practically independent of m_h, and reads

$$\mu_{\text{eff}}\,\frac{\tan\beta}{50} \;\lesssim\; 4.1\,\text{TeV}\times\left(\frac{m_{\tilde{\tau}_1}}{150\,\text{GeV}}\right)\,. \tag{13}$$

We find that the annihilation channel into Higgs pairs relative to the annihilation into gauge bosons can well be larger by factors of $\mathcal{O}(10^3)$ without violating the unitarity bound (13).

4 Primordial staus

4.1 BBN constraints

Various cosmological constraints on the stau yield $Y_{\tilde{\tau}} \equiv Y_{\tilde{\tau}^+} + Y_{\tilde{\tau}^-}$ have been explored in the literature. In a scenario where the LSP is very weakly coupled, the NLSP decays a considerable time after the start of BBN. The decay products of such long-lived particles can alter the primordial light element abundances. This leads to constraints on the released electromagnetic and hadronic energy [40–42]. The constraints on the stau relic abundance from decays depend on the stau lifetime and mass as well as on the electromagnetic and hadronic branching ratios. For reasonable values of the stau mass, the hadronic branching fraction is typically $\lesssim \mathcal{O}(10^{-3})$ which leads to rather weak constraints. Stronger constraints come from electromagnetic energy injection, especially at late times. Here the bounds can be as strong as $m_{\tilde{\tau}} Y_{\tilde{\tau}} \lesssim 10^{-13}$ GeV [43]. However, typically the stau NLSP abundance and lifetime can satisfy the limits obtained from BBN by considering NLSP decays alone [3, 15, 19, 23–28]

In addition to injecting energetic showers into the plasma through decays, negatively charged particles can form bound states with light nuclei, which can lead to a drastic overproduction of ^{6}Li [29] and ^{9}Be [44]. This leads to strong constraints on the stau yield $Y_{\tilde{\tau}^-}$ for lifetimes longer than a few thousand seconds. While [45] gives a rather conservative upper bound of $Y_{\tilde{\tau}^-} \lesssim 10^{-14}$ derived from ^{6}Li alone, [44] takes into account ^{6}Li as well as ^{9}Be leading to $Y_{\tilde{\tau}^-} \lesssim 10^{-15}$ which translates into $Y_{\tilde{\tau}} \lesssim 2\cdot 10^{-15}$ in the absence of a stau anti-stau asymmetry.

4.2 Stau relic abundance

The relic abundance of a (meta)stable particle can be calculated using the Boltzmann equation. For the stau yield $Y_{\widetilde{\tau}}$, (again in the absence of a stau anti-stau asymmetry) it takes the form [46]

$$\frac{\mathrm{d}Y_{\widetilde{\tau}}}{\mathrm{d}x} \;=\; -\sqrt{\frac{2g_*}{45}}\,\pi\,M_{\mathrm{P}}\,\frac{m_{\widetilde{\tau}_1}}{x^2}\,\langle\sigma_{\mathrm{ann}}\,v\rangle\,\left(Y_{\widetilde{\tau}}^2 - Y_{\widetilde{\tau},\mathrm{eq}}^2\right)\;, \tag{14}$$

where $M_{\mathrm{P}} = 2.43\cdot 10^{18}\,\mathrm{GeV}$ is the reduced Planck mass, $Y_{\widetilde{\tau},\mathrm{eq}}^2$ is the abundance in thermal equilibrium and $g_* \simeq 85$ represents the effective number of degrees of freedom at the stau freeze out (cf. [46]).

It is well known that the relic abundance of a (meta)stable particle is inversely proportional to its annihilation cross section times its mass (see e.g. [35]). In the case where the stau freeze-out is dominated by the Higgs channel, we can write the solution to (14) as

$$Y_{\widetilde{\tau}} \;=\; 10^{-15}\left(\frac{10^{-5}\,\mathrm{GeV}^{-2}}{\langle\sigma v\rangle}\right)\left(\frac{200\,\mathrm{GeV}}{m_{\widetilde{\tau}_1}}\right)\;. \tag{15}$$

If stau and Higgs are not mass degenerate ($m_{\widetilde{\tau}_1} - m_h \gtrsim 5\,\mathrm{GeV}$), the annihilation cross section (5) is practically independent of m_h and depends only on the stau mass $m_{\widetilde{\tau}_1}$ and the stau-Higgs coupling $\propto \mu\,\tan\beta\,\sin 2\theta_{\widetilde{\tau}} = \mu_{\mathrm{eff}}\,\tan\beta$. Our result for the yield can then be written as

$$Y_{\widetilde{\tau}} = 1.4\cdot 10^{-15}\left(\frac{m_{\widetilde{\tau}_1}}{150\,\mathrm{GeV}}\right)^5\left(\frac{1\,\mathrm{TeV}}{\mu}\right)^4\left(\frac{50}{\tan\beta}\right)^4\left(\frac{1}{\sin 2\theta_{\widetilde{\tau}}}\right)^4\;. \tag{16}$$

Here we neglected subleading effects of the order 10 % like e.g. Sommerfeld enhancement.[2] Combining our result (16) with the unitarity bound (13) we find that the lowest allowed abundance is $Y^{\mathrm{min}} \sim 4\cdot 10^{-18}$ for $m_{\widetilde{\tau}_1} = 120\,\mathrm{GeV}$. As explained in Section 3, the minimal, theoretically viable abundance might well turn out to be larger than this value. From the conservative bound (10) we infer however that nevertheless $Y^{\mathrm{min}} \lesssim 10^{-15}$.

4.3 A comment on stau asymmetries

So far we have assumed that there is no asymmetry in the stau sector, that is, there are as many $\widetilde{\tau}^+$ as $\widetilde{\tau}^-$ degrees of freedom. On the other hand, a large class of baryogenesis mechanisms rely on $(B+L)$ violation by sphalerons [48, 49], which leads to an excess of baryons over anti-baryons if there are more anti-leptons than leptons. In particular, leptogenesis [12] falls into this class. From this point of view it appears natural to assume that there is also an asymmetry in the slepton sector at the time of stau annihilation and freeze out. Now it is important to distinguish between slepton number conserving and slepton number violating annihilation processes (Figure 2).

[2] See e.g. [47] for an explanation of the Sommerfeld effect and an estimate of the errors in the general case of a charged relic.

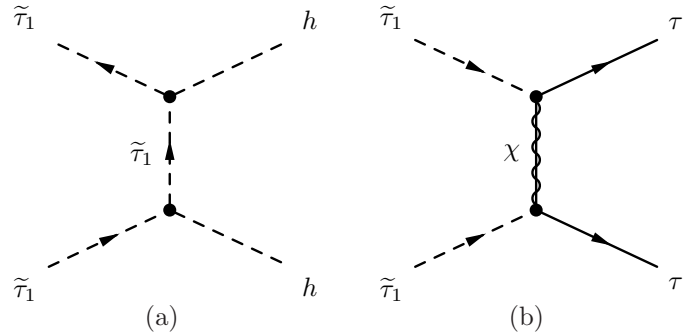

Figure 2: Examples for slepton number conserving (a) and violating (b) annihilation processes.

As we have seen, in settings with substantial left-right mixing in the stau sector, the slepton number conserving processes dominate over the violating ones. On the other hand, the slepton number violating processes are still effective until the stau relic abundance has reached a value $Y_{\widetilde{\tau}} \sim 10^{-12} \ldots 10^{-13}$ [22]. It is then clear that if the slepton asymmetry in the stau sector is of the order of the baryon asymmetry, $\eta_b \sim 10^{-10}$, asymmetries will play no role. However, if there are order one asymmetries in the (s)tau sector, this might have important implications for the relic abundance of $\widetilde{\tau}^-$: in a situation in which there is a large excess of $\widetilde{\tau}^+$ over $\widetilde{\tau}^-$, the remaining $\widetilde{\tau}^-$ are more likely to find an annihilation partner, and hence their relic abundance can get suppressed more strongly. For stau lifetimes where electromagnetic bounds are not overly restrictive, $\tau_{\widetilde{\tau}} \lesssim 10^7\,\mathrm{s}$, a relatively large abundance of $\widetilde{\tau}^+$, $Y_{\widetilde{\tau}^+} \lesssim 10^{-13}$, can still be consistent with BBN because they do not form bound states with nuclei.

5 Scenarios with low $Y_{\widetilde{\tau}}$

In this section we present some 'top-down motivated settings' in which the previously discussed strong suppression of the stau relic abundance occurs. If a scenario can have a large stau annihilation cross section is fully determined by the stau spectrum. The necessary conditions are:

Condition 1: Substantial left-right mixing of the stau mass eigenstates $\widetilde{\tau}_1$ and $\widetilde{\tau}_2$ driven by a large off-diagonal stau mass matrix element $m^2_{\widetilde{\tau}_{\mathrm{LR}}} \simeq -m_\tau\,\mu\,\tan\beta$. This requires large μ and $\tan\beta$.

Condition 2: Moderate $m_{\widetilde{\tau}_1}$, preferably $m_{\widetilde{\tau}_1} \lesssim 200\,\mathrm{GeV}$.

We will check these conditions by looking at the entries of the stau mass matrix $m^2_{\widetilde{\tau}_{\mathrm{R}}}$, $m^2_{\widetilde{\tau}_{\mathrm{L}}}$ and $m^2_{\widetilde{\tau}_{\mathrm{LR}}}$ as well as on the mass eigenvalues $m_{\widetilde{\tau}_1}$ and $m_{\widetilde{\tau}_2}$.

It is clear that we could simply write down the desired stau mass matrices. The purpose of this section however is to present soft mass patterns defined at the unification scale M_{GUT} that lead to mass matrices with the above properties. To this end, it is useful to recall the (one-loop) renormalization group equations (RGEs) for the stau soft masses

(see e.g. [35])

$$8\pi^2 \frac{\mathrm{d}m^2_{\tilde{\tau}_{\mathrm{L\,soft}}}}{\mathrm{d}t} = y_\tau^2 S_\tau - 3g_2^2 |M_2|^2 - g_Y^2 |M_1|^2 - \frac{1}{2} g_Y^2 S_Y \,, \tag{17a}$$

$$8\pi^2 \frac{\mathrm{d}m^2_{\tilde{\tau}_{\mathrm{R\,soft}}}}{\mathrm{d}t} = 2\, y_\tau^2 S_\tau - 4\, g_Y^2 |M_1|^2 + g_Y^2 S_Y \,, \tag{17b}$$

where

$$S_\tau = m^2_{H_1} + m^2_{\tilde{\tau}_{\mathrm{L\,soft}}} + m^2_{\tilde{\tau}_{\mathrm{R\,soft}}} + |A_\tau|^2 \,, \tag{18a}$$

$$S_Y = \frac{1}{2} \sum_i Y_i\, m_i^2 \tag{18b}$$

with Y_i denoting the hypercharge of the scalar i. Note that $m^2_{\tilde{\tau}_{\mathrm{L}}} \simeq m^2_{\tilde{\tau}_{\mathrm{L\,soft}}}$ and $m^2_{\tilde{\tau}_{\mathrm{R}}} \simeq m^2_{\tilde{\tau}_{\mathrm{R\,soft}}}$ as other contributions are tiny (cf. (21)).

In order to obtain large mixing (condition 1) we have to demand that the right-hand sides (rhs) of (17) be similar, assuming coincident stau masses at the high scale. In addition, we need a large off-diagonal stau mass. $|\mu|$ which determines the size of $m^2_{\tilde{\tau}_{\mathrm{LR}}}$ together with $\tan\beta$ is fixed at the weak scale by the condition of correct electroweak symmetry breaking which reads (at tree-level) [35]

$$|\mu|^2 = \frac{m^2_{H_2} \sin^2\beta - m^2_{H_1} \cos^2\beta}{\cos 2\beta} - \frac{M_Z^2}{2} \overset{\text{large } \tan\beta}{\simeq} -m^2_{H_2} \,. \tag{19}$$

An unsuppressed $m^2_{\tilde{\tau}_{\mathrm{LR}}}$ can typically be realized for $\mu \sim 1 - 2\,\mathrm{TeV}$. In principle it is not difficult to get μ in this range, however one should mention here that a relatively large μ might be associated with a significant amount of electroweak fine-tuning as can be seen from (19).In addition, very large values for μ might lead to charge breaking vacua with unacceptably short lifetimes (cf. Section 3).

The second condition is already partially fulfilled if the mixing is sizable. To further reduce the stau masses, the rhs of (17) should not be too negative.

In what follows we present three scenarios where the desired stau mass patterns arise and low relic abundances through the Higgs channel can be achieved. We use micrOMEGAs 2.0.7 [50,51] to calculate the relic abundance of the stau NLSP numerically. The superpartner spectrum is determined by SOFTSUSY 2.0.18 [52] whereas the Higgs mass is calculated with the specialized tool FeynHiggs 2.5.1 [53–56]. For the top quark pole mass, we use the latest best-fit value of 172.6 GeV [57]. Experimental constraints on the parameter space arise primarily through mass limits. We employ the LEP Higgs bound $m_h \geq 114\,\mathrm{GeV}$ and $m_{\tilde{\tau}_1} \geq 100\,\mathrm{GeV}$ [58]. Theoretical constraints, as discussed in Section 3, are not shown explicitly.

5.1 CMSSM with large $\tan\beta$

Let us start with the constrained supersymmetric standard model (CMSSM), which is defined through its free parameters $m_{1/2}$, m_0, A_0, $\tan\beta$ and $\mathrm{sign}\,\mu$. Although we will

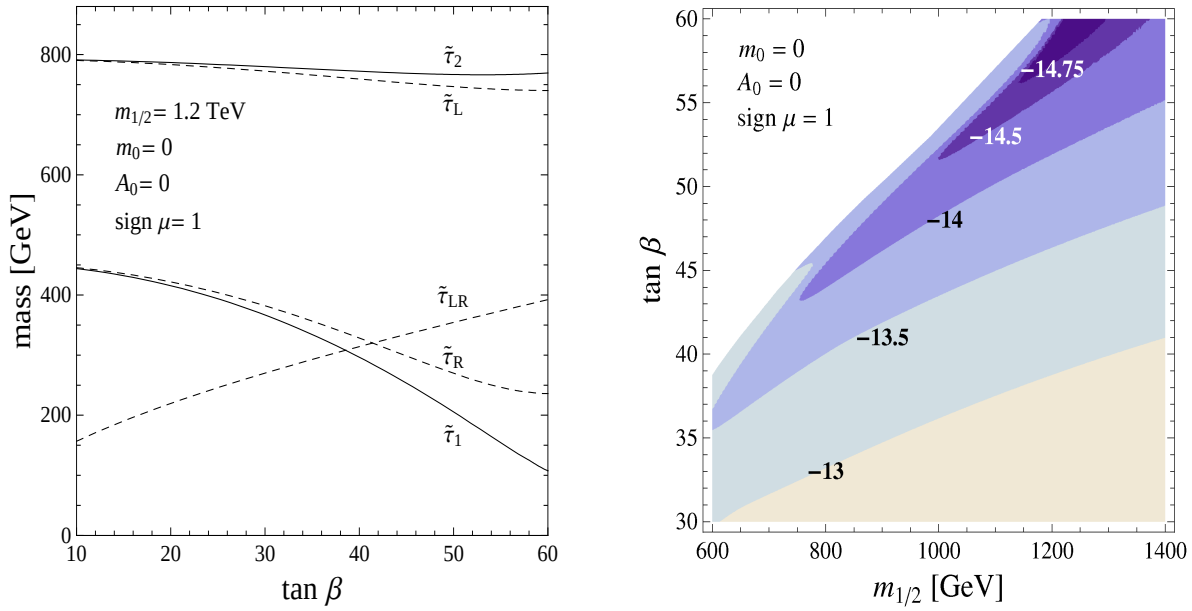

Figure 3: Stau relic abundance in the CMSSM. The left panel shows the dependence of the left- and right-handed stau masses, the off-diagonal mass and the mass eigenvalues on $\tan\beta$. In the right panel we plot the logarithm of the stau relic abundance $\log_{10}(Y_{\tilde{\tau}})$ in the $(m_{1/2} - \tan\beta)$ –plane. We find the minimal yield to be around $Y_{\tilde{\tau}}^{\rm min} \simeq 10^{-15}$. The white region in the right panel is excluded due to direct searches.

see that the annihilation can be more efficient in other scenarios, we find it nevertheless worthwhile to point out that also in this scheme a major suppression of the relic abundance is possible. The important quantity here is $\tan\beta$ which we plot against the stau spectrum in the left panel of Figure 3 for a typical stau NLSP parameter point.

The plot shows that $m_{\tilde{\tau}_{\rm R}}$ and $m_{\tilde{\tau}_1}$ decrease strongly with $\tan\beta$ through the tau Yukawa term in the RGE of $m^2_{\tilde{\tau}_{\rm R\,soft}}$, because $y_\tau \propto \tan\beta$. Since μ is practically independent of $\tan\beta$ the off-diagonal mass[3] $m_{\tilde{\tau}_{\rm LR}}$ grows like $\sqrt{\tan\beta}$ which leads to a further reduction of $m_{\tilde{\tau}_1}$ through left right-mixing. However, in spite of a strong off-diagonal stau mass, mixing cannot get close to maximal, because of a large difference $m^2_{\tilde{\tau}_{\rm L}} - m^2_{\tilde{\tau}_{\rm R}}$. We conclude that condition 2 can easily be satisfied while condition 1 only partially. In summary, we obtain a significant enhancement of the stau annihilation cross section through the Higgs channel at large $\tan\beta$ which is however limited by the mixing angle. To illustrate the effect, Figure 3 shows the stau relic abundance in the CMSSM as a function of $\tan\beta$.

5.2 Non-universal Higgs masses (NUHM)

In the NUHM we can vary – in addition to the parameters of the CMSSM – the down- and up-type soft Higgs masses squared at the GUT scale, $m^2_{H_1}$ and $m^2_{H_2}$. We employ the GUT scale stability constraint $m^2_{H_{1,2}} + |\mu^2| \geq 0$ to avoid dangerous vacua and electroweak

[3] We use the definition $m_{\tilde{\tau}_{\rm LR}} = \sqrt{|m^2_{\tilde{\tau}_{\rm LR}}|}$ in the following.

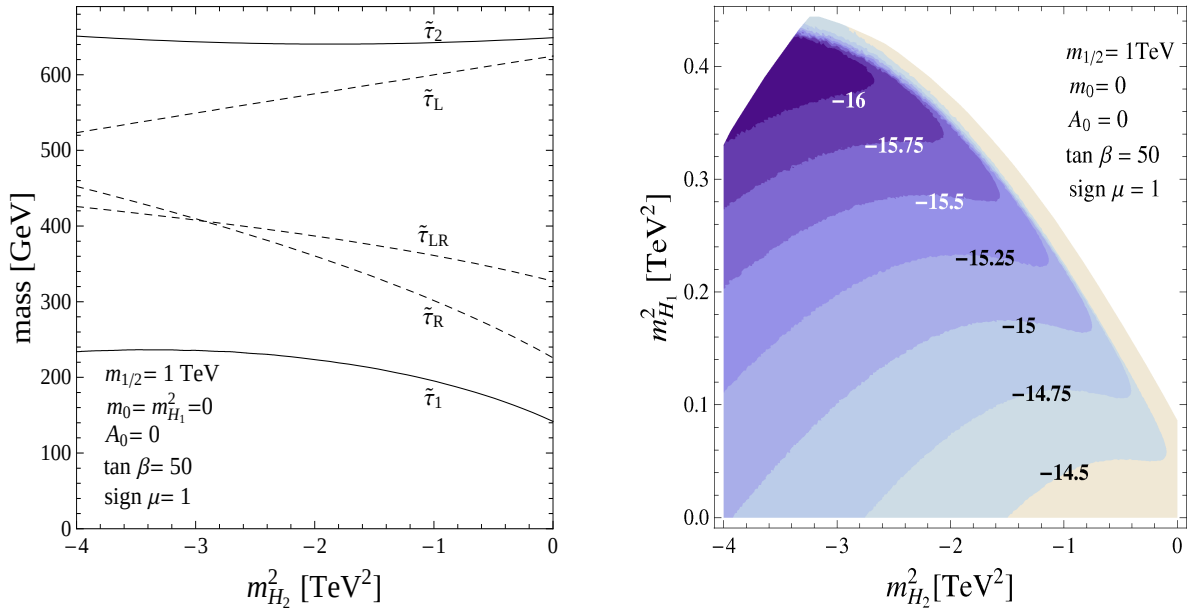

Figure 4: Stau relic abundance in the NUHM. The left panel shows the dependence of the left- and right-handed stau masses, the off-diagonal mass and the mass eigenvalues on the soft Higgs mass $m^2_{H_2}$. In the right panel we plot the logarithm of the stau relic abundance $\log_{10}(Y_{\tilde{\tau}})$ for different $m^2_{H_1}$ and $m^2_{H_2}$. Some of the low $\tilde{\tau}$ yield regions might be excluded by theoretical constraints (cf. Section 3). Again, the white region in the right panel is excluded.

symmetry breaking at the GUT scale [59]. It is instructive to investigate the additional effects on the stau spectrum compared to the CMSSM which arise through the variation of the soft Higgs masses: increasing $m^2_{H_1}$ leaves $m_{\tilde{\tau}_{LR}}$ unchanged, but it reduces $m_{\tilde{\tau}_L}$ and $m_{\tilde{\tau}_R}$ dominantly through the Yukawa term in the soft mass RGEs (17) which contains $m^2_{H_1}$. However more interesting for us is the impact of $m^2_{H_2}$ which we show in the left panel of Figure 4. We observe that a growth of $m^2_{H_2}$ reduces $m_{\tilde{\tau}_R}$ and enlarges $m_{\tilde{\tau}_L}$. As $m^2_{H_2}$ does not appear in the Yukawa term of the RGEs (17), this effect arises through the S_Y-term. For the off-diagonal stau mass $m_{\tilde{\tau}_{LR}}$, it is important to recall that $|\mu^2| \simeq -m^2_{H_2}$ at the weak scale, cf. (19). Therefore, increasing $m^2_{H_2}$ leads to a suppression of $m^2_{\tilde{\tau}_{LR}}$.

The low yield parameter region is at relatively large negative $m^2_{H_2}$, where the GUT stability constraint can still be satisfied and again at large $\tan\beta$. Here both, the left-right mixing as well as the off-diagonal stau mass $m_{\tilde{\tau}_{LR}}$, can further be enhanced compared to the CMSSM case. Stau masses which are slightly larger can be reduced by a positive $m^2_{H_1}$. We conclude that both conditions can be satisfied in this region, leading to an extremely suppressed stau abundance.

5.3 Scenarios with non-universal gaugino masses (NUGM)

The possibility of having non-universal gaugino masses as high scale boundary conditions even for unified theories has been realized long ago [60]. For concreteness we focus here on SU(5) GUTs and assume that supersymmetry be broken by F-term vacuum expectation values of chiral fields. These fields have to transform as the symmetric

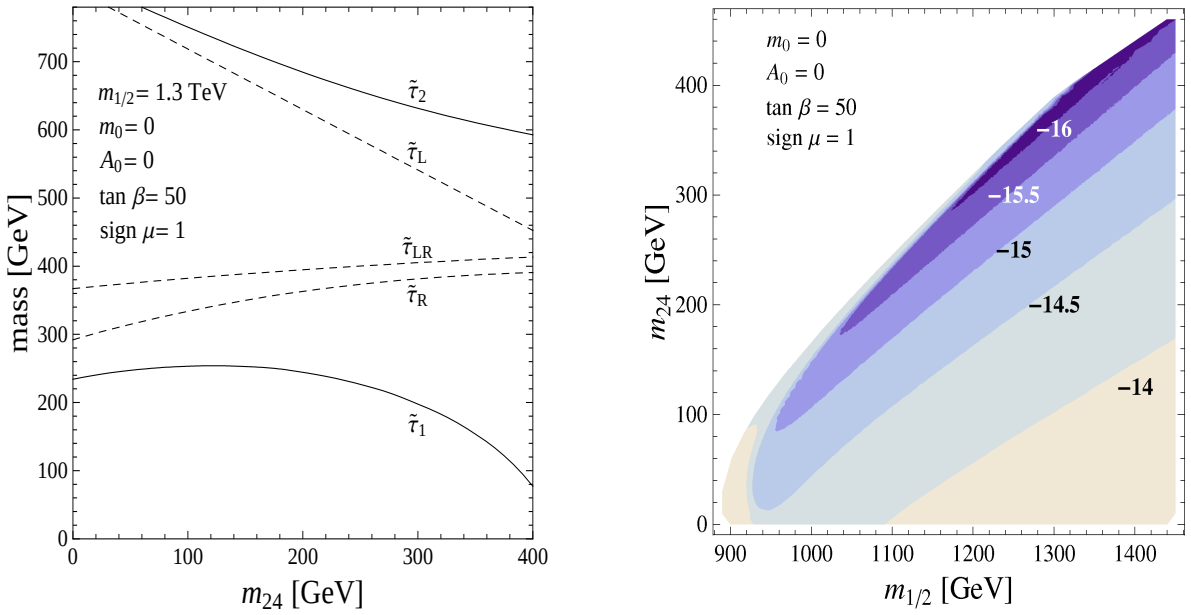

Figure 5: Stau relic abundance in the NUGM. The left panel shows the dependence of the left- and right-handed stau masses, the off-diagonal mass and the mass eigenvalues on m_{24}. In the right panel we plot the logarithm of the stau relic abundance $\log_{10}(Y_{\tilde{\tau}})$ in the $(m_{1/2} - m_{24})$ –plane. Some of the low $\tilde{\tau}$ yield regions might be excluded by theoretical constraints (cf. Section 3). Once more, the white region in the right panel is excluded.

product of two adjoint representations of the GUT group, but not necessarily as singlets. In the following we concentrate on the two smallest possible representations for the supersymmetry breaking fields, which are simply the singlet and the **24**plet.

The high-scale mass patterns of the gauginos of $\mathrm{SU}(3)_C$, $\mathrm{SU}(2)_\mathrm{L}$ and $\mathrm{U}(1)_Y$ turn out to be given as linear combinations of singlet ($m_{1/2}$) and **24**plet (m_{24}) contributions [61],

$$\begin{aligned} M_1 &= m_{1/2} - 0.5\, m_{24}\ , \\ M_2 &= m_{1/2} - 1.5\, m_{24}\ , \\ M_3 &= m_{1/2} + m_{24}\ . \end{aligned} \tag{20}$$

The only new parameter compared to the CMSSM is the mass arising from the **24**plet, m_{24}. Its impact on the stau spectrum is illustrated in the left panel of Figure 5.

$m_{\tilde{\tau}_\mathrm{L}}$ decreases quickly for growing m_{24} as the smaller M_2 reduces the $\mathrm{SU}(2)_\mathrm{L}$ gauge contribution to $m^2_{\tilde{\tau}_{\mathrm{L\,soft}}}$. $m_{\tilde{\tau}_\mathrm{R}}$ increases slightly, although the $\mathrm{U}(1)_Y$ gauge contribution to $m^2_{\tilde{\tau}_{\mathrm{R\,soft}}}$ shrinks. This is because the reduction of $m^2_{\tilde{\tau}_{\mathrm{R\,soft}}}$ through the Yukawa term in (17b) is less effective for smaller $m^2_{\tilde{\tau}_{\mathrm{L\,soft}}}$. The off-diagonal mass matrix entry $m^2_{\tilde{\tau}_\mathrm{LR}} \propto \mu$ grows slowly as μ gets a contribution from the increasing gluino mass M_3.

It turns out that diagonal and off-diagonal stau soft masses can come very close, leading to maximal left-right mixing in the stau sector with a strong reduction of $m_{\tilde{\tau}_1}$ driven by a large $m_{\tilde{\tau}_\mathrm{LR}}$. As this is the key ingredient for strongly enhanced couplings of $\tilde{\tau}_1$ to the light Higgs, the stau relic abundance becomes very small, as can be seen in the right panel of Figure 5.

5.4 Further remarks

Let us briefly summarize the main results of this section. We have seen that a strong suppression of the stau relic abundance can be achieved such that all cosmological constraints can be evaded. We also checked that the shown regions of parameter space are not in conflict with precision measurements of $b \to s\,\gamma$ and the Tevatron limit of $B_s \to \mu^+\mu^-$. Furthermore, the parameter regions with low relic abundance are all within the $2\,\sigma$ interval of the measured anomalous magnetic moment of the muon, the only exception being the CMSSM for $m_{1/2} \gtrsim 1100\,\text{GeV}$. Comparing the low yield regions with the CBBN bound $Y_{\widetilde{\tau}} \lesssim 2 \cdot 10^{-15}$ we see that even in the CMSSM there remains some viable region in parameter space while for the NUHM and NUGM the stau relic abundance can be even smaller. Further analysis of the experimental signatures of such low stau yield regions appears desirable.

6 Prospects for the LHC

A very appealing property of our scenario is that it will be tested at the LHC. Given the stau spectrum, the stau-Higgs coupling is fully determined. It is then easy to see the impact of the Higgs channel for stau annihilation in the early universe.

A common feature of the low yield regions is a rather small stau mass, $m_{\widetilde{\tau}_1} \lesssim 250\text{GeV}$, while the other SUSY particles may be quite heavy. In general, the prospects for the LHC depend mainly on the mass scale of the colored superpartners. If they are not too heavy, as can be the case e.g. in the NUHM, they will be produced in large numbers at the LHC due to their large cross sections. In this case one has a good chance to measure the whole SUSY spectrum in the cascade decays of gluinos and squarks and it should not be too difficult to extract information about the stau-Higgs coupling.

If, however, the mass scale of colored particles exceeds $2 - 2.5\,\text{TeV}$, their production will become very rare or even impossible at the LHC [62]. But even in this case, being rather light, staus could still be pair produced, e.g. in the Drell-Yan process $q\,\bar{q} \to \widetilde{\tau}_1^-\,\widetilde{\tau}_1^+$ through a virtual photon or Z boson [63]. The number of produced stau pairs for different stau masses are shown in Table 1. Further details on the stau spectrum might be extracted from the Drell-Yan production of $\widetilde{\tau}_1\,\widetilde{\nu}_\tau$, $\widetilde{\tau}_1\,\widetilde{\tau}_2$ and $\widetilde{\tau}_2\,\widetilde{\tau}_2$, if kinematically accessible.

Mass	150 GeV	200 GeV	300 GeV	400 GeV
$\#_{\widetilde{\tau}_\text{R}}$	2000	800	200	60
$\#_{\widetilde{\tau}_\text{L}}$	6000	2000	450	150

Table 1: Estimated number of produced stau pairs in Drell-Yan processes at the LHC for integrated luminosity of $100\,\text{fb}^{-1}$ extracted from Figure 1 of [64]. The number of produced mass eigenstates depends on the mixing angle and should lie in between the values given for left- and right-handed staus.

Another interesting pair production mechanism in our scenario is gluon-gluon fusion.

Here two gluons generate a fermion loop (preferably a top-loop) to which a virtual Higgs boson is attached which finally decays into a stau pair. In an early study [65] the cross section for this process was found to be three orders of magnitude below the corresponding Drell-Yan cross section. Note that in our scenario, due to the strong stau-Higgs coupling, this suppression can at least partially be compensated such that gluon-gluon fusion could be comparable to the Drell-Yan process.

Altogether we see that even in scenarios in which some superpartners are beyond the reach of the LHC, one may nevertheless establish the existence of supergravity in nature along the lines of [1–9].

7 Conclusions

We have analyzed stau NLSP scenarios. In contrast to previous studies, we have not assumed that the stau mass eigenstates be purely right- or left-handed, but have allowed for non-trivial left-right mixing. In the case of substantial mixing, the annihilation into Higgs bosons can dominate over other channels, such that the thermal relic stau abundance, i.e. the abundance obtained without invoking late-time entropy production, can be strongly reduced. This makes it possible to evade all BBN constraints. The emerging scenarios have the advantage that they allow for rather large reheating temperatures, as required for instance by leptogenesis, and the cold dark matter can be explained in terms of 'thermally' produced gravitinos. Most importantly, all ingredients of our low stau yield scenarios will be tested at the LHC.

Acknowledgments

We would like to thank Alejandro Ibarra and David Straub for useful discussions. We are indebted to the referee for important comments on an earlier version of this paper. This work has been supported by the SFB-Transregio 27 "Neutrinos and Beyond" and by the DFG cluster of excellence "Origin and Structure of the Universe".

A Stau Masses & Mixings

Let us briefly introduce our conventions concerning the masses and mixings of the stau. We assume that there is no mixing between different slepton generations and take μ and A^τ to be real parameters, such the stau mass matrix can be written as

$$\begin{aligned}\mathcal{M}^2_{\widetilde{\tau}} &= \begin{pmatrix} m^2_{\widetilde{\tau}_{\mathrm{L\,soft}}} + (\sin^2\theta_{\mathrm{W}} - \frac{1}{2})M_Z^2\cos 2\beta + m_\tau^2 & -m_\tau(A^\tau + \mu\tan\beta) \\ -m_\tau(A^\tau + \mu\tan\beta) & m^2_{\widetilde{\tau}_{\mathrm{R\,soft}}} - \sin^2\theta_{\mathrm{W}} M_Z^2\cos 2\beta + m_\tau^2 \end{pmatrix} \\ &\equiv \begin{pmatrix} m^2_{\widetilde{\tau}_{\mathrm{L}}} & m^2_{\widetilde{\tau}_{\mathrm{LR}}} \\ m^2_{\widetilde{\tau}_{\mathrm{LR}}} & m^2_{\widetilde{\tau}_{\mathrm{R}}} \end{pmatrix} . \end{aligned} \tag{21}$$

A non-zero off-diagonal element $m^2_{\widetilde{\tau}_{\rm LR}}$ leads to a mixing of the chiral states $\widetilde{\tau}_{\rm L}$ and $\widetilde{\tau}_{\rm R}$. We can diagonalize the stau mass matrix by an orthogonal transformation

$$\mathcal{O}^{\mathcal{T}}\,\mathcal{M}^2_{\widetilde{\tau}}\,\mathcal{O} \;=\; \begin{pmatrix} m^2_{\widetilde{\tau}_1} & 0 \\ 0 & m^2_{\widetilde{\tau}_2} \end{pmatrix} . \tag{22}$$

The mass eigenvalues are

$$m^2_{\widetilde{\tau}_{1,2}} \;=\; \frac{1}{2}\left[m^2_{\widetilde{\tau}_{\rm L}} + m^2_{\widetilde{\tau}_{\rm R}} \mp \sqrt{(m^2_{\widetilde{\tau}_{\rm L}} - m^2_{\widetilde{\tau}_{\rm R}})^2 + 4m^4_{\widetilde{\tau}_{\rm LR}}} \right] . \tag{23}$$

The orthogonal 2×2 matrix $\mathcal{O}$ is parameterized by the stau left-right mixing angle $\theta_{\widetilde{\tau}}$, which relates the mass eigenstates and the chiral states,

$$\begin{pmatrix} \widetilde{\tau}_1 \\ \widetilde{\tau}_2 \end{pmatrix} \;=\; \begin{pmatrix} \cos\theta_{\widetilde{\tau}} & \sin\theta_{\widetilde{\tau}} \\ -\sin\theta_{\widetilde{\tau}} & \cos\theta_{\widetilde{\tau}} \end{pmatrix} \begin{pmatrix} \widetilde{\tau}_{\rm L} \\ \widetilde{\tau}_{\rm R} \end{pmatrix} . \tag{24}$$

The mixing angle $\theta_{\widetilde{\tau}}$ is given by

$$\cos\theta_{\widetilde{\tau}} \;=\; \frac{-m^2_{\widetilde{\tau}_{\rm LR}}}{\sqrt{(m^2_{\widetilde{\tau}_{\rm L}} - m^2_{\widetilde{\tau}_1})^2 + m^4_{\widetilde{\tau}_{\rm LR}}}} . \tag{25}$$

References

[1] W. Buchmüller, K. Hamaguchi, M. Ratz, and T. Yanagida, Phys. Lett. **B588** (2004), 90, hep-ph/0402179.

[2] W. Buchmüller, K. Hamaguchi, M. Ratz, and T. Yanagida, hep-ph/0403203.

[3] J. L. Feng, S. Su, and F. Takayama, Phys. Rev. **D70** (2004), 075019, hep-ph/0404231.

[4] A. Brandenburg, L. Covi, K. Hamaguchi, L. Roszkowski, and F. D. Steffen, Phys. Lett. **B617** (2005), 99, hep-ph/0501287.

[5] K. Hamaguchi, Y. Kuno, T. Nakaya, and M. M. Nojiri, Phys. Rev. **D70** (2004), 115007, hep-ph/0409248.

[6] J. L. Feng and B. T. Smith, Phys. Rev. **D71** (2005), 015004, hep-ph/0409278.

[7] H.-U. Martyn, hep-ph/0605257.

[8] J. R. Ellis, A. R. Raklev, and O. K. Øye, hep-ph/0607261.

[9] R. Kitano, arXiv:0806.1057 [hep-ph].

[10] J. E. Kim and H. P. Nilles, Phys. Lett. **B138** (1984), 150.

[11] G. F. Giudice and A. Masiero, Phys. Lett. **B206** (1988), 480.

[12] M. Fukugita and T. Yanagida, Phys. Lett. **B174** (1986), 45.

[13] S. Davidson and A. Ibarra, Phys. Lett. **B535** (2002), 25, hep-ph/0202239.

[14] M. Bolz, A. Brandenburg, and W. Buchmüller, Nucl. Phys. **B606** (2001), 518, hep-ph/0012052.

[15] J. Pradler and F. D. Steffen, Phys. Lett. **B648** (2007), 224, hep-ph/0612291.

[16] I. V. Falomkin et al., Nuovo Cim. **A79** (1984), 193, [Yad. Fiz. **39** (1984), 990].

[17] M. Y. Khlopov and A. D. Linde, Phys. Lett. **B138** (1984), 265.

[18] J. R. Ellis, J. E. Kim, and D. V. Nanopoulos, Phys. Lett. **B145** (1984), 181.

[19] D. G. Cerdeño, K.-Y. Choi, K. Jedamzik, L. Roszkowski, and R. Ruiz de Austri, JCAP **0606** (2006), 005, hep-ph/0509275.

[20] T. Kanzaki, M. Kawasaki, K. Kohri, and T. Moroi, Phys. Rev. **D75** (2007), 025011, hep-ph/0609246.

[21] L. Covi and S. Kraml, JHEP **08** (2007), 015, hep-ph/0703130.

[22] T. Asaka, K. Hamaguchi, and K. Suzuki, Phys. Lett. **B490** (2000), 136, hep-ph/0005136.

[23] M. Fujii, M. Ibe, and T. Yanagida, Phys. Lett. **B579** (2004), 6, hep-ph/0310142.

[24] J. R. Ellis, K. A. Olive, Y. Santoso, and V. C. Spanos, Phys. Lett. **B588** (2004), 7, hep-ph/0312262.

[25] K. Jedamzik, K.-Y. Choi, L. Roszkowski, and R. Ruiz de Austri, JCAP **0607** (2006), 007, hep-ph/0512044.

[26] F. D. Steffen, JCAP **09** (2006), 001, hep-ph/0605306.

[27] W. Buchmüller, L. Covi, J. Kersten, and K. Schmidt-Hoberg, JCAP **0611** (2006), 007, hep-ph/0609142.

[28] R. H. Cyburt, J. Ellis, B. D. Fields, K. A. Olive, and V. C. Spanos, JCAP **0611** (2006), 014, astro-ph/0608562.

[29] M. Pospelov, Phys. Rev. Lett. **98** (2007), 231301, hep-ph/0605215.

[30] W. Buchmüller, K. Hamaguchi, M. Ibe, and T. T. Yanagida, Phys. Lett. **B643** (2006), 124, hep-ph/0605164.

[31] K. Hamaguchi, T. Hatsuda, M. Kamimura, Y. Kino, and T. T. Yanagida, Phys. Lett. **B650** (2007), 268, hep-ph/0702274.

[32] F. Takayama and M. Yamaguchi, Phys. Lett. **B485** (2000), 388, hep-ph/0005214.

[33] W. Buchmüller, L. Covi, K. Hamaguchi, A. Ibarra, and T. Yanagida, JHEP **03** (2007), 037, hep-ph/0702184.

[34] J. Kersten and K. Schmidt-Hoberg, JCAP **0801** (2008), 011, arXiv:0710.4528 [hep-ph].

[35] M. Drees, R. Godbole, and P. Roy, Hackensack, USA: World Scientific (2004).

[36] S. R. Coleman, Phys. Rev. **D15** (1977), 2929.

[37] A. Kusenko, P. Langacker, and G. Segre, Phys. Rev. **D54** (1996), 5824, hep-ph/9602414.

[38] P. M. Ferreira, Phys. Lett. **B512** (2001), 379, hep-ph/0102141.

[39] K. Griest and M. Kamionkowski, Phys. Rev. Lett. **64** (1990), 615.

[40] R. H. Cyburt, J. R. Ellis, B. D. Fields, and K. A. Olive, Phys. Rev. **D67** (2003), 103521, astro-ph/0211258.

[41] M. Kawasaki, K. Kohri, and T. Moroi, Phys. Rev. **D71** (2005), 083502, astro-ph/0408426.

[42] K. Jedamzik, Phys. Rev. **D74** (2006), 103509, hep-ph/0604251.

[43] M. Kawasaki, K. Kohri, and T. Moroi, Phys. Lett. **B649** (2007), 436, hep-ph/0703122.

[44] M. Pospelov, J. Pradler, and F. D. Steffen, arXiv:0807.4287 [hep-ph].

[45] K. Jedamzik, arXiv:0710.5153 [hep-ph].

[46] P. Gondolo and G. Gelmini, Nucl. Phys. **B360** (1991), 145.

[47] C. F. Berger, L. Covi, S. Kraml, and F. Palorini, arXiv:0807.0211 [hep-ph].

[48] F. R. Klinkhamer and N. S. Manton, Phys. Rev. **D30** (1984), 2212.

[49] V. A. Kuzmin, V. A. Rubakov, and M. E. Shaposhnikov, Phys. Lett. **B155** (1985), 36.

[50] G. Belanger, F. Boudjema, A. Pukhov, and A. Semenov, Comput. Phys. Commun. **149** (2002), 103, hep-ph/0112278.

[51] G. Belanger, F. Boudjema, A. Pukhov, and A. Semenov, Comput. Phys. Commun. **176** (2007), 367, hep-ph/0607059.

[52] B. C. Allanach, Comput. Phys. Commun. **143** (2002), 305, hep-ph/0104145.

[53] S. Heinemeyer, W. Hollik, and G. Weiglein, Comput. Phys. Commun. **124** (2000), 76, hep-ph/9812320.

[54] S. Heinemeyer, W. Hollik, and G. Weiglein, Eur. Phys. J. **C9** (1999), 343, hep-ph/9812472.

[55] G. Degrassi, S. Heinemeyer, W. Hollik, P. Slavich, and G. Weiglein, Eur. Phys. J. **C28** (2003), 133, hep-ph/0212020.

[56] M. Frank et al., JHEP **02** (2007), 047, hep-ph/0611326.

[57] CDF, arXiv:0803.1683 [hep-ex].

[58] LEPSUSYWG, ALEPH, DELPHI, L3, and OPAL experiments, note LEPSUSYWG/02-05.1, (http://lepsusy.web.cern.ch/lepsusy/Welcome.html).

[59] J. R. Ellis, T. Falk, K. A. Olive, and Y. Santoso, Nucl. Phys. **B652** (2003), 259, hep-ph/0210205.

[60] J. R. Ellis, K. Enqvist, D. V. Nanopoulos, and K. Tamvakis, Phys. Lett. **B155** (1985), 381.

[61] K. Huitu, T. Kobayashi, K. Puolamaki, and Y. Kawamura, Prepared for EPS-HEP 99, Tampere, Finland, 15-21 Jul 1999.

[62] H. Baer, C. Balazs, A. Belyaev, T. Krupovnickas, and X. Tata, JHEP **06** (2003), 054, hep-ph/0304303.

[63] E. Eichten, I. Hinchliffe, K. D. Lane, and C. Quigg, Rev. Mod. Phys. **56** (1984), 579.

[64] G. Bozzi, B. Fuks, and M. Klasen, Phys. Lett. **B609** (2005), 339, hep-ph/0411318.

[65] F. del Aguila and L. Ametller, Phys. Lett. **B261** (1991), 326.